ICAS-86-4.8.3

# RESEARCH ON ACTIVE SUPPRESSION TECHNOLOGY FOR WING/AILERON FLUTTER

D.M. Zhu, Z.Q. Gu, M.H. Can

Z.F. Chen and W.P. Wang

Nanjing Aeronautical Institute

Nanjing, China

## Abstract

In this paper investigation is made into the active suppression technology of wing/aileron flutter. The combination of analytical methods with experimental approach to establish mathematical models for servo-aeroelastic systems, the use of sub-optimal output feedback control theory to synthesize control laws for wing/aileron flutter, the ground and wind-tunnel experimental techniques of aeroelastic systems are discussed.

## Nomenclature

$A$ Controller dynamics matrix
$A_i$ Generalized aerodynamic coefficient matrix
$A_a$ Dynamics matrix for actuator
$A_g$ Dynamics matrix for gust model
$B= B_oB_c$ Controller input matrix
$B_a$ Input matrix for actuator
$B_g$ Input matrix for gust model
$b_o$ Half reference chord length
$C$ Controller output matrix
$C_a$ Output matrix for actuator
$C_g$ Output matrix for gust model
$C_p$, $M_p$, $K_p$ Generalized structural damping, mass and stiffness matrices
$C_s$ Sensive coefficient matrix of sensors
$C_y$ Output modal matrix
$D_i$ Generalized aerodynamic coefficient matrix for control surface
$E_i$ Generalized aerodynamic coefficient matrix for gust input
$E(.)$ Expected value of (.)
$F_s$ Servo-aeroelastic dynamics matrix
$G_a$ Augmented input matrix
$G_u$ Servo-aeroelastic input matrix
$G_w$ Gust noise input matrix
$J_s$ Performance index (PI)
$m$ Number of control surface
$M_{p\beta}$ Inertial coupling matrix
$n$ Number of aerodynamic approximation terms
$N$ Order of the plant
$N_c$ Order of controller
$N_g$ Order of gust model
$N_f$ Number of structural modes
$q=\rho V^2/2$ Dynamic pressure
$R_{uo}$ Input noise intensive matrix
$R_{yo}$ Measurement noise intensive matrix
$R_w$ Gust noise intensive matrix
$r$ Number of sensors
$\bar{s}=sV/b_o$
$s$ Laplace variable
$tr(.)$ Trace of matrix (.)
$u$ Actuator input signal
$u_c$ Controller output signal
$u_o$ Plant input noise
$V$ Flight velocity
$x_a$ Augmented state vector
$x_c$ Controller state vector
$x_p$ Generalized coordinate vector
$x_g$ Gust state vector
$x_s$ Plant state vector
$y_o$ Measurement noise vector
$y_s$ Plant output vector
$z_i$ Displacement of measured point i
$\beta$ Generalized coordinate for control surface deflection
$w$ Vertical gust white noise
$\Lambda$ Lagrange multiplier matrix
$\rho$ Air density
$(\dot{})$ Time derivative

## I. Introduction

A considerable amount of research has been made in the application of active controls to increase aircraft flutter velosity. In the past, analytical and experimental work on active wing/aileron flutter suppression has produced promising results and demonstrated its potential for providing significant improvements on aircraft performance. But in a number of cases, a wing/aileron flutter will take place when the operating system can not provide sufficient stiffness for the aileron. The wing/aileron flutter is a significant factor in degrading the speed performance of a aircraft.

This paper will discuss the active suppression technology for wing/aileron flutter by the way of analytic and experimental techniques. Special attention of research is paid to three aspects: the establishment of mathematical model for servo-aeroelastic systems, the design of active flutter suppression control laws, and the testing of flutter control system.

Of the three aspects, the synthesis of active flutter control laws is the most important one. In recent years, synthesizing control laws with the optimal control theory has got much benefit, and become more and more popular. At the beginning, the design approach is that an optimal state feedback control law or a Kalman's filter was first synthesized and then the practical low-order control law was obtained by the transfer function matching technique or modal residulization method. The direct method of synthesizing low-order optimal output feedback control laws had not been studied until the beginning of 80' s. (1) However, even for the direct method (2,3), two essential problems still exist: one is the selection of initial values for the controller and the convegence of iteration; the other is the lack of any theoretical guarantee of the stability of closed-loop control system. This paper, based on the specialities of aeroelastics, and the demands for flutter control system properties, presents a gradually-changing-parameter design method of sub-optimal output feedback control laws for active flutter suppression which, as shown, can be used to synthesize flutter control laws directly without the above-mentioned problems.

As this study shows, the technology of active flutter suppression including analysis and experiment procedures presented in this paper is practical and efficient.

## II. Wind-Tunnel Test Model

The test specimen in this paper is the wind-tunnel model of a triangle wing with low-aspect ratio. The wing model is cantilevered from the tunnel floor, and has a soft-supported outboard aileron and a control surface in the middle of the wing trailing edge which is driven by an electrohydraulic servo-actuator system. The general configuration and photograph of the model installed in the wind-tunnel are presented in Fig. 1.

### Structure

The model is of conventional spar and pod construction, that is, an aluminun spar is used to provide bending and torsional stiffness with span-wise section and pods to provide aerodynamic contours. Lead blocks are fixed on spar nodes to simulate structural mass distribution.

For aeroelastic analysis purpose, the first 5 elastic mode shapes, frequencies and structural dampings of the wing model were obtained from ground vibration tests. The natural frequencies and dampings of the first 5 modes are presented in Table 1. As shown, the second mode is the outboard aileron roll with the frequency $7.26H_z$.

### Control Surface and Actuator

The model is equipped with a trailing-edge control surface which is located between 28.4 percent and 58.4 percent semi-span stations and is approximately 25 percent of the local wing chord. The control surface is driven by an electrohydraulic servo-actuator system. The actuator serves two purposes: for no command, it fixes the control surface position relative to the wing; and for time varying inputs, it drives the control surface in a manner dictated by the control law. Maximum control surface rotation is approximately $\pm 8^{\circ}$.

For analysis purpose, the actuator frequency response was experimentally measured by fast sinuous sweep-frequency testing technique, and approximated by a transfer function in Laplace plane :

$$\frac{\beta(s)}{u(s)} = \frac{4.769\times10^5}{s^3+241.1s^2+1.919\times10^5 s+3.212\times10^7} \quad \text{rad/v} \qquad (1)$$

Open-loop wind-tunnel test

The wind-tunnel flutter test of the wing without control system was carried out in the $2.5\times3m^2$ low-speed wind tunnel of Nanjing Aeronautical Institute. This test had two purposes: to obtain the open-loop flutter velocity and frequency; and to measure the frequency response function of the wing so as to modify the analytical model of the actuator-wing system later.

As the time constant of aeroelastic system is usually relative large, the technique of external steady excitation and double-channel FFT analyser was used to improve the signal-noise ratio and to suppress random noise and harmonic components. During the test the actuator was used as excitor. The acceleration responses of the wing on station 1 at two diffirent velocities are presented in Fig. 2. The testing results showed that the flutter velocity and frequency of the wing were 20.6 m/sec and 6.2 Hz correspondingly. The flutter mode is the coupling between the first bending of the wing and the elastic rotation of the aileron.

Aerodynamics

The unsteady aerodynamics for the first 5 modes and control surface rotation mode were computed by using a doublet-lattice aerodynamics computer program. The variations of the unsteady aerodynamics in frequency were approximated with a rational polynomial in the variable s by the way of Roger's approximation.

State equation and open-loop analysis

As shown in Appendix A, the equation of motion of the wing could be written as a set of first-order linear ordinary differential equations of the form:

$$\dot{x}_s = F_s x_s + G_u u + G_w w, \quad x_s \in R^N, \ u \in R^m$$
$$y_s = H_s x_s + y_o, \qquad y_s, y_o \in R^r \qquad (2)$$

The eigenvalues of Eqs. (2) as a function of velocity shown in Fig. 3 (arrows indicate increasing velocity) reveal that the wing/aileron flutter occurs at a airflow speed of 19.8 m/sec and a frequency of 6.24 Hz. The results compared favorably with the test ones.

As shown in Fig.3, there is a higher frequency flutter mode which involves primarily the first torsion of the wing and is stable to a relatively higher velocity of 39.0 m/sec.

III. Sub-optimal Control Formulation

A controller model is assumed as (Fig.4)

$$\dot{x}_c = Ax_c + By_s, \quad x_c \in R^{N_c}$$
$$u_c = Cx_c, \qquad u_c \in R^m \qquad (3)$$

By defining an augmented state vector

$$x_a = \begin{Bmatrix} x_s \\ x_c \end{Bmatrix}$$

the closed-loop control system is represented by the augmented state equation

$$x_a = F_a x_a + G_a \eta_a \qquad (4)$$

with

$$\eta_a = \begin{Bmatrix} u_o \\ w \\ y_o \end{Bmatrix}$$

and

$$F_a = \begin{bmatrix} F_s & G_u C \\ BH_s & A \end{bmatrix}; \qquad G_a = \begin{bmatrix} G_u & G_w & 0 \\ 0 & 0 & B \end{bmatrix}$$

Usually, the control law is determined by using an optimal method to search for design variables in matrices A,B and C which minimizes the performance index (PI) defined by

$$J_s(A,B,C)= \tfrac{1}{2}E(y_s^T Q_1 y_s + u^T Q_2 u) = \tfrac{1}{2}tr( Q_a X_a ) \qquad (5)$$

with

$$Q_a = \begin{bmatrix} H_s^T Q_1 H_s & 0 \\ 0 & C^T Q_2 C \end{bmatrix}$$

$$X_a = E(x_a x_a^T)$$

In order to secure the convergence of iteration in obtaining the optimal control law from the above equations and the stability of closed-loop control system, an unequal constraint equation is used to modify the above optimal output feedback control problem

$$g_s(A,B,C) = \max_i \mathrm{Re}\{\lambda_i(F_a)\} < -\sigma, \ \sigma > 0 \qquad (6)$$

with $\lambda_i(F_a)$ representing i-th eigenvalue of matrix $F_a$ . It is obvious that $g_s(A,B,C)$ equals the maximum real part of all augmented eigenvalues and that to satisfy inequality (6) means to have a stability margin $\sigma$ at least for closed-loop control system.

Since the optimal solution of Eq. (5) with unequal constraint (6) is usually different with original optimal solution, it is supposed to call above optimal problem (5) with inequality (6) as sub-optimal output feedback control method.

The sub-optimal control problem can be solved with the Feasible Direction Method. By using Lagrange multiplier method to treat the equal constraints, the necessary conditions for minimizing $J_s$ is

$$\begin{aligned} F_a X_a + X_a F_a^T + G_a R_a G_a^T &= 0 \\ F_a^T \Lambda + \Lambda F_a + Q_a &= 0 \end{aligned} \qquad (7)$$

with $\Lambda$ being non-negative Lagrange multiplier matrix and $R_a$ being augmented noise intensive matrix

$$R_a = \begin{bmatrix} R_{uo} & 0 & 0 \\ 0 & R_w & 0 \\ 0 & 0 & R_{yo} \end{bmatrix}$$

To partition matrices $X_a$ and $\Lambda$ as

$$X = \begin{bmatrix} X_s & X_{sc} \\ X_{sc}^T & X_c \end{bmatrix}$$

$$\Lambda = \begin{bmatrix} \Lambda_s & \Lambda_{sc} \\ \Lambda_{sc}^T & \Lambda_c \end{bmatrix}$$

we obtain the partial-differential matrices of $J_s$ (PI) as

$$\frac{\partial J_s}{\partial A} = \Lambda_{sc}^T X_{sc} + \Lambda_s X_c$$

$$\frac{\partial J_s}{\partial B} = (\Lambda_{sc}^T X_s + \Lambda_c X_{sc}^T) H_s^T + \Lambda_c B R_{yo} \qquad (8)$$

$$\frac{\partial J_s}{\partial C} = Q_2 C X_c + G_u^T (\Lambda_s X_{sc} + \Lambda_{sc} X_c)$$

## IV. Computation Method for Control Laws of Active Flutter Suppression

### Design Variables

There are several possible ways of choosing a set of $N_c(m+r)$ design variables in the controller matrices A,B and C. In order to get a controller order as low as possible and make control system have good dynamic performance, it is practically convinent to choose a same filter for all feedback pathes. In this case, the controller model is represented by

$$\dot{x}_c = Ax_c + B_o B_c y_s \qquad (9)$$
$$u_c = Cx_c$$

where

$B_o$ a column vector of $N_c$ dimension

$B_c$ a row vector of r dimension

For reducing difficulties of realizing an optimal control law, the elements in matrices A,B. and C can be pre-determined by practical needs for filters before an optimal program starts. So only the elements in matrix $B_c$ are chosen as free design variables and the differential matrix of (PI) $J_s$ is now simplified as

$$\frac{dJ_s}{dB_c} = B_o^T( {}^T_{sc}X_s + {}_c X_{sc}^T)H_s^T + (B_o^T \, {}_c B_o)B_c R_{yo} \qquad (10)$$

### Algorithm

Knowing the performance index, gradient and unequal constraint, an optimization procedure called the Feasible Direction Method can be used to obtain the sub-optimal output feedback control law. From the stability characteristics of a aircraft via its flight velocity, a gradually-changing-parameter design for synthesizing suboptimal output control law of active flutter suppression can be successfully performed without the difficulties of choosing initial controller values and securing convergence of each iteration. Also, the resulting closed-loop control system will have good stability margin in the flight envelope.

The design algorithm consists of the following steps:

1. Choose the highest design velocity $V_d$, which is higher than the open-loop flutter velocity $V_{fo}$. and a initial starting design velocity $V_1$ lower than $V_{fo}$. Set the initial controller design variables as

$$B_c = 0$$
and $j = 1$;

2. Solve sub-optimal control problem at velocity $V_1$ by

(1) Setting

$$\sigma_{j,o} = -g_s(B_c) \quad \text{and } i=0;$$

(2) Obtaining $X_{a,i+1}$ and $\Lambda_{i+1}$ from Lyapunov equations

$$F_{a,i}X_{a,i+1} + X_{a,i+1}F_{a,i}^T + G_{a,i}R_a G_{a,i}^T = 0$$
$$F_{a,i}^T\Lambda_{i+1} + \Lambda_{i+1}F_{a,i} + Q_{a,i} = 0$$

(3) obtaining new control law from Eq. (10)

$$B_{c,new} = -(B_o^T\Lambda_{c,i+1}B_o)^{-1}B_o^T(\Lambda_{sc,i+1}^T X_{s,i+1} + \Lambda_{c,i+1}X_{sc,i+1}^T)H_s^T R_{yo}^{-1}$$

and defining a new matrix gradients:

$$d(B_{c,i}) = B_{c,new} - B_{c,i}$$

(4) computing

$$B_{c,i+1} = B_{c,i} + \alpha_{i+1}d(B_{c,i})$$

where $\alpha_{i+1}$, lying in the interim (0,1), is chosen so that the matrix $B_{c,i+1}$ satisfies the following inequality:

$$g_s(B_{c,i+1}) < -\sigma_i$$

(5) calculating the performance index

$$J_{s,i+1} = \tfrac{1}{2}tr(Q_a X_{a,i+1})$$

and norm

$$\delta_{i+1} = \left\| \frac{dJ_s}{dB_c} \right\|_i$$

If $\left| \frac{J_{s,i+1} - J_{s,i}}{J_{s,i}} \right| < \varepsilon_1$ and

$$\left| \frac{\delta_{i+1} - \delta_i}{\delta_i} \right| < \varepsilon_2 ,$$

set the sub-optimal output feedback control law at present design velocity $V_j$ as

$$B_{c,sub}^{(j)} = B_{c,i+1}$$

Otherwise, set

$$\sigma_{i+1} = -g_s(B_{c,i+1}) \ , \ i=i+1$$

return to step (2).

3. If $V_j = V_d$, stop the calculation and **set the sub-optimal control law of** active flutter suppression in whole flight envelope of the aircraft as

$$B_{c,sub} = B_{c,\ sub}^{(j)}$$

Otherwise, choose a new design velocity $V_{j+1}$ between $V_j$ and $V_d$ so that the closed-loop control system with control law

$$u(s)=C(sI-A)^{-1}B_o B_{c,sub}^{(j)} \ y_s(s)$$

is stable and the initial controller values at the velocity $V_{j+1}$ can be set as

$$B_{c,o}^{(j+1)} = B_{c,sub}^{(j)}$$

Set $V_j=V_{j+1}$ and $j=j+1$ .

Return to step 2.

## V. Flutter Suppression Control law

In our wind-tunnel entry, the sensors were three accelerometers embeded in the wing structure at the points 1, 2 and 3 (see Fig. 1). Based on the analyzing the open-loop frequency response (see Fig.2), the dynamic feedback network used to suppress the wing/aileron flutter is predetermined as a filter of 4th order defined by

$$A=\begin{bmatrix} -20 & 1 & 0 & 0 \\ -1200 & -20 & 0 & 0 \\ 1600 & 0 & -30 & 0 \\ 480 & 0 & 21 & -60 \end{bmatrix}, \quad B_o=\begin{bmatrix} 0 \\ 1 \\ 0 \\ 0 \end{bmatrix}$$

$$C=\begin{bmatrix} 288 & 0 & 12.6 & 24 \end{bmatrix}$$

In the present analysis, three accelerometers are used as feedback signals of the servo-aeroelastic system. The gradually-changing-parameter design approach of sub-optimal flutter control laws is used to determine the matrix $B_c$ in the controller (9). The result is

$$B_c = \begin{bmatrix} -1.3878 & 3.4235 & 0.8380 \end{bmatrix}$$

Fig. 5 shows a root locus of the closed loop control system with airspeed as a parameter. The flutter speed of the wing with the above controller is about 29 m/s, which is 45% higher than that of the open-loop system. Moreover the flutter mode of the wing with the controller is the first torsion of the wing instead of the coupling of the first wing bending and the aileron rotation in the open-loop case.

As shown in Fig. 6, the Nyquist plot of the closed-loop system at three velocities of airflow which are 20%, 25% and 30% higher than the flutter velosity of the open-loop system seperately, the closed loop control system has good stability margins for both gains and phase and has robust stability in response to the variation of the velocity of airflow.

## VI. Conclusion

The direct method called as the gradually-changing-parameter design method presented in this paper offers a systematic method of synthesizing a low-order suboptimal output feedback control law for active flutter suppression. By introducing an unequal constraint, which represents the stability margin of an aircraft, into optimal output feedback control theory, a nonlinear programming algorithm is employed to search for the control law design variables that minimize a performance index defined by a weighted sum of mean square steady output responses and control inputs directly without the difficulties of choosing initial values of the control law and securing convergence of each iteration.

The method is applied to wing/aileron flutter suppression of a servo-aeroelastic wing model represented by a 35th order system. A fourth order control law is synthesized by using the signals of three accelerameters as output feedback signals. The results indicate that the control law performs well at both design and off-design flight velocities and has good stability margins in the whole flight envelope, that demonstrates its insensitivity to flight condition and the flutter velocity of closed loop system is 45% higher than the one of open-loop system.

## References


1. Newsom, J.R., A Method for Obtaining Practical Flutter Suppression Control Laws Using Results of Optimal Control Theory, NASA TP-1471, 1979

2. Mukhopadhyay, V., Newsom, J.R. and Abel, I., A Direct Method for Synthesizing Low-order Optimal Feedback Control Laws with Application to Flutter Suppression, AIAA 80-1613, 1980

3. Mukhopadhyay, V., Newsom, J.R. and Abel, I., A Method for Obtaining Reducing-Order Control Laws for High-Order Systems Using Optimization Techniques, NASA TP-1876, 1981


## Appendix A

### State Equation Of The Wing Model

The model motion equation representing a flexible aircraft in flight is

$$(M_p s^2 + C_p s + K_p) x_p(s) + M_{p\beta}\beta(s) = q(\{A_0:D_0:E_0\} + \{A_1:D_1:E_1\}\bar{s} + \{A_2:D_2E_2\}\bar{s}^2 + \sum_{i=3}^{n} \frac{\bar{s}}{\bar{s}+r_i}\{A_i:D_i:E_i\})\begin{Bmatrix} x_p(s) \\ \beta(s) \\ w_g(s)/V \end{Bmatrix} \quad \text{(A-1)}$$

From the transfer function of servo-actuator, the standard realization for actuator is:

$$\dot{x} = A_a x + B_a u \quad \text{(A-2)}$$

with

$$x = \begin{Bmatrix} \beta \\ \dot{\beta} \\ \ddot{\beta} \end{Bmatrix}$$

A turbulence model represented by the following second-order transfer function is used to approximate to a Dryden gust spectrum

$$\frac{w_g(s)}{w(s)} = \frac{\sigma_{wg}\sqrt{3V/l}\,(s+V/\sqrt{3}\,l)}{(s+V/l)^2} \quad \text{(A-3)}$$

where

$\sigma_{wg}$ root-mean-square gust velocity

$l$ scale of turbulence or characteristic length (m)

For numerical calculation $l=30.48$ m and $\sigma_{wg} = 1$ m/sec. The model of disturbance can be expressed as a Markov's process

$$\dot{x}_g = A_g x_g + B_g w, \qquad y_g = C_g x_g \quad \text{(A-4)}$$

with

$$x_g = \begin{Bmatrix} w_g/V \\ \dot{w}_g/V \end{Bmatrix}; \quad y_g = \begin{Bmatrix} w_g/V \\ \dot{w}_g/V \\ \ddot{w}_g/V \end{Bmatrix}$$

By introducing generalized aerodynamics state vectors defined by

$$x_{vi}(s) = \frac{\bar{s}}{\bar{s}+r_i}\{A_i x_p(s) + D_i\beta(s) + E_i w_g/V\}; \quad i=3,\ldots,n \quad \text{(A-5)}$$

we obtain the state equation of the servo-aeroelastic system:

$$\dot{x}_s = F_s x_s + G_u u + G_w w \qquad (A-6)$$

where

$$x_s = \{ x_p^T, \dot{x}_p^T, x_{v3}^T, \ldots, x_{vn}^T, x^T, x_g^T \}^T$$

$$F_s = \begin{bmatrix} F & B_v & B_w C_g \\ 0 & A_a & 0 \\ 0 & 0 & A_g \end{bmatrix}$$

$$Gu = \begin{Bmatrix} 0 \\ B_a \\ 0 \end{Bmatrix}; \quad Gw = \begin{Bmatrix} 0 \\ 0 \\ B_g \end{Bmatrix}$$

$$B_v = \left[\begin{array}{c|c|c} 0 & 0 & 0 \\ \hline qM^{-1}D_o & qM^{-1}D_1/\bar{V} & qM^{-1}D_2/\bar{V}^2 - M^{-1}M_{p\beta} \\ \hline 0 & qD_3 & 0 \\ \hline \vdots & \vdots & \vdots \\ \hline 0 & qD_n & 0 \end{array}\right]$$

$$B_w = \left[\begin{array}{c|c|c} 0 & 0 & 0 \\ \hline qM^{-1}E_o & qM^{-1}E_1/\bar{V} & qM^{-1}E_2/\bar{V} \\ \hline 0 & qE_3 & 0 \\ \hline \vdots & \vdots & \vdots \\ \hline 0 & qE_n & 0 \end{array}\right]$$

$$F = \left[\begin{array}{c|c|c|c|c} 0 & I & 0 & \ldots & 0 \\ \hline -M^{-1}K' & -M^{-1}C' & M^{-1} & \ldots & M^{-1} \\ \hline 0 & qA_3 & -r_3\bar{V}I & \ldots & 0 \\ \hline \vdots & \vdots & \vdots & \ldots & \vdots \\ \hline 0 & qA_n & 0 & \ldots & -r_n\bar{V}I \end{array}\right]$$

$$M = M_p - qA_2/\bar{V}^2$$

$$C' = C_p - qA_1/\bar{V}$$

$$K' = K_p - qA_o$$

$$\bar{V} = V/b_o$$

## Appendix B

### Output Equation of The Wing Model

The response at the station k on flexible aircraft can be expressed by mode-superposition method as

$$z_k = \sum_{i=1}^{N_f} c_{ki} x_{pi} \; ; \qquad (B-1)$$

If r acceleration sensors are used to measure motion signals at r stations of an aircraft, the output equation can be written as

$$y_s = C_s \begin{Bmatrix} z_1 \\ z_2 \\ \vdots \\ z_r \end{Bmatrix} = C_s C_y x_p \qquad (B-2)$$

By substituting Eqs. (A-6) into Eq.(B-2) and considering the measurement noise represented by an output noise vector $y_o$, the output equation of the flexible aircraft can expressed as

$$y_s = H_s x_s + y_o \qquad (B-3)$$

where

$$H_s = C_s C_y M^{-1} [ -K' \vdots -C' \vdots I \vdots \ldots \vdots I \vdots D \vdots D_g C_g ]$$

$$D = [ qD_o : qD_1/\bar{V} : qD_2/\bar{V}^2 - M_{p\beta} ]$$

$$D_g = [ qE_o : qE_1/\bar{V} : qE_2/\bar{V}^2 ]$$

$C_s$ sensive coefficient matrix of the sensors

$C_y$ output modal matrix

| | Mode 1 | Mode 2 | Mode 3 | Mode 4 | Mode 5 |
|---|---|---|---|---|---|
| Frequency (HZ) | 4.36 | 7.26 | 12.9 | 20.2 | 21.0 |
| Damping Ratio | 0.0091 | 0.0081 | 0.0080 | 0.0168 | 0.0121 |

Table 1 Structural Mode Parameters of the Wing

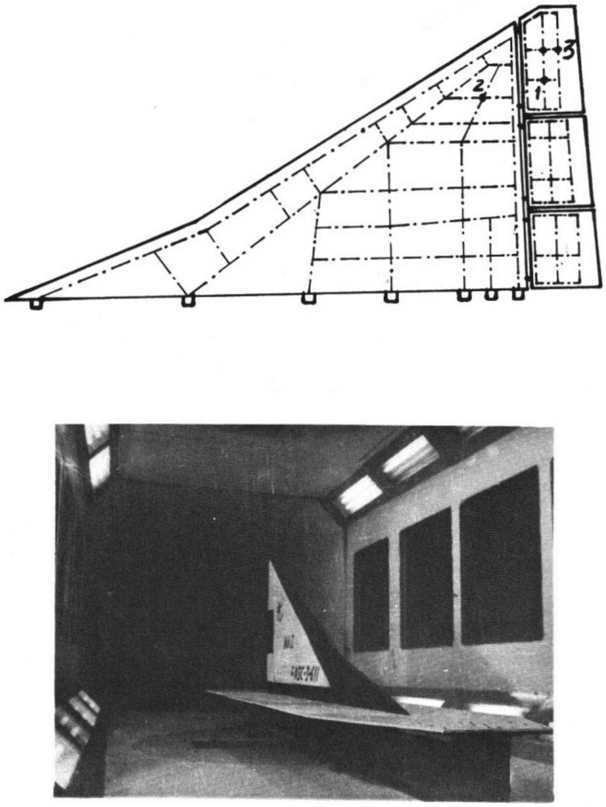

Fig. 1 Wind-tunnel test model of wing

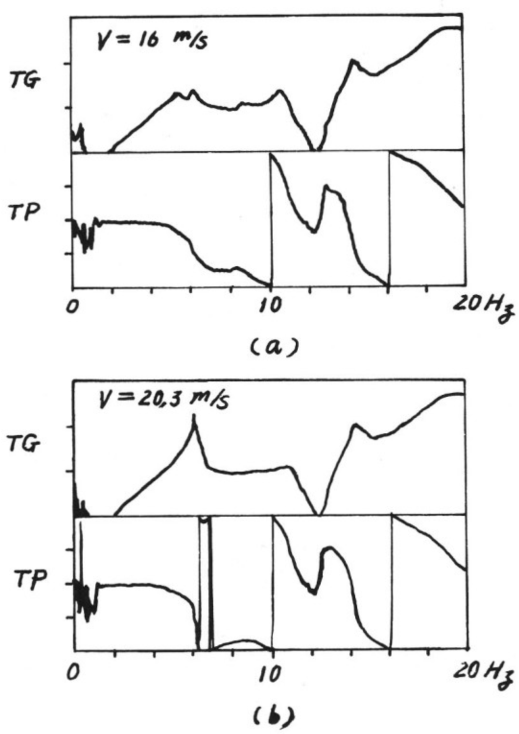


Fig. 2 Acceleration frequency response of wing at station 1

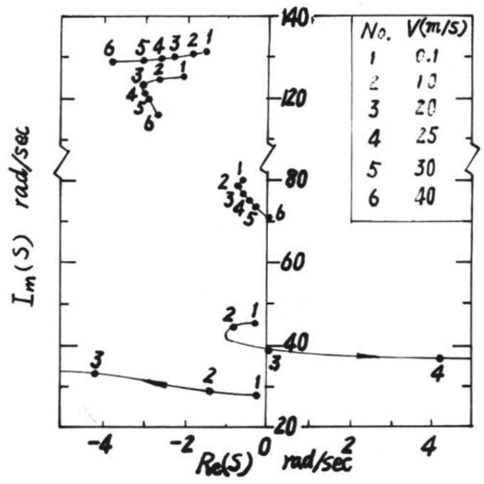


Fig. 3 Open-loop velocity root locus

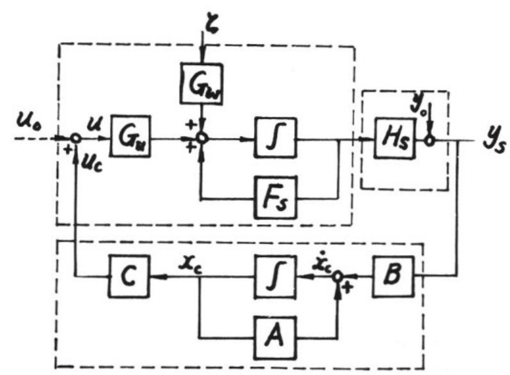


Fig.4 Block diagram of control system

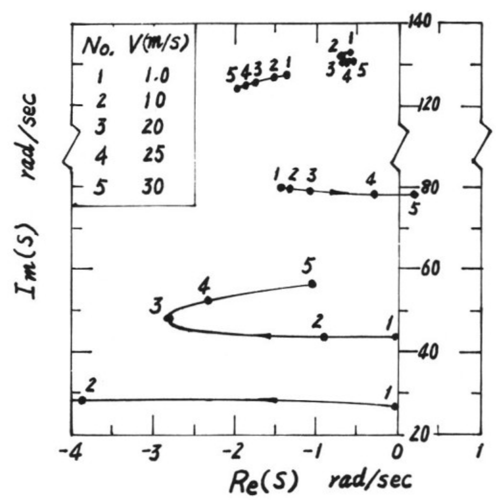


Fig. 5 Closed-loop velocity root locus

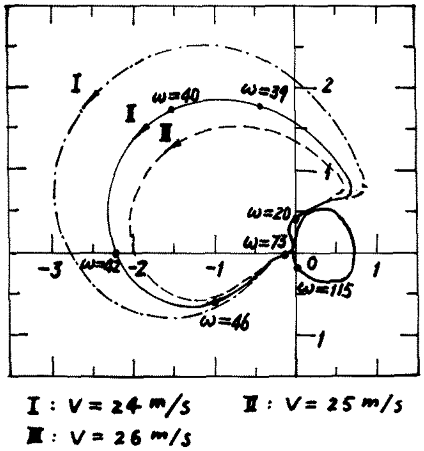


Fig.6 Nyquist plot of closed-loop system